Meteoritics & Planetary Science 35, 215–227 (2000)

Complexly zoned chromium-aluminum spinel found *in situ* in the Allende meteorite

S. B. SIMON[1]*, K. D. McKEEGAN[2], D. S. EBEL[1] AND L. GROSSMAN[1,3]

[1]Department of the Geophysical Sciences, 5734 South Ellis Avenue, The University of Chicago, Chicago, Illinois 60637, USA
[2]Department of Earth and Space Sciences, University of California, Los Angeles, Los Angeles, California 90095, USA
[3]The Enrico Fermi Institute, 5640 South Ellis Avenue, The University of Chicago, Chicago, Illinois 60637, USA
*Correspondence author's e-mail address: sbs8@midway.uchicago.edu

(Received 1999 May 18; accepted in revised form 1999 October 5)

Abstract–In addition to the Mg-, Al-, ^{16}O-rich spinels that are known to occur in refractory inclusions, the Murchison meteorite contains Cr-rich, ^{16}O-poor spinels, most of whose sources are unknown because they are rarely found *in situ*. Here we report the *in situ* occurrence in Allende of Cr-rich spinels, found in 13 chondrules and 4 "olivine-rich objects". The Allende spinels exhibit major and minor element contents, isotopic compositions, and zoning of Cr_2O_3 contents like those of the Cr-spinels from Murchison. Some chondrules contain patchy-zoned spinel (Simon *et al.*, 1994), which suggests that such grains did not form by sintering but perhaps by formation of overgrowths on relic grains. Unlike the olivine-rich objects, phases in all three chondrules that were analyzed by ion microprobe have uniform, near-normal O-isotopic compositions. One olivine-rich object, ALSP1, has a huge (1 mm) fragment of chevron-zoned spinel. This spinel has near-normal O-isotopic compositions that are quite distinct from those of adjacent forsteritic olivine, which are relatively ^{16}O-rich and plot on the calcium-aluminum-inclusion (CAI) line, like some isolated forsterite grains found in Allende. The spinel and olivine in this object are therefore not genetically related to each other. Another olivine-rich object, ALSP11A, contains a rectangular, 150 × 100 μm, homogeneous spinel grain with 50 wt% Cr_2O_3 and 23 wt% FeO in a vuggy aggregate of finer-grained (5–90 μm), FeO-rich (Fo_{47-55}) olivine. The magnesian core of one olivine grain has a somewhat ^{16}O-rich isotopic composition like that of the large spinel, whereas the FeO-rich olivine is relatively ^{16}O-poor. The composition of the spinel in ALSP11A plots on the CAI line, the first Cr-rich spinel found to do so. Chevron-zoned spinel has not been observed in chondrules, and it is unlikely that either ALSP1 or ALSP11A were ever molten. Calculations show that a spinel with the composition of that in ALSP1 can condense at 1780 K at a P^{tot} of 10^{-3} atm and a dust/gas ratio of 100 relative to solar. The Cr-rich spinel in ALSP11A could condense at ~1420 K, but this would require a dust/gas enrichment of 1000 relative to solar. The data presented here confirm that, as in Murchison, the coarse Cr-rich spinels in Allende are relatively ^{16}O-depleted and are isotopically distinct from the ^{16}O-enriched $MgAl_2O_4$ from CAIs. Sample ALSP11A may represent a third population, one that is Cr-rich and plots on the CAI line. That the O-isotopic composition of ALSP1 is like those of Cr-rich spinels from chondrules indicates that O-isotopic compositions cannot be used to distinguish whether grains from such unequilibrated objects are condensates or are fragments from a previous generation of chondrules.

INTRODUCTION

Unzoned Mg-Al spinel grains from calcium-aluminum-rich inclusions (CAIs) found in carbonaceous chondrites such as Murchison (CM2) and Allende (CV3) are ^{16}O-rich, with $\delta^{18}O$ and $\delta^{17}O$ typically between –40 and –50‰ (Clayton *et al.*, 1977; Clayton and Mayeda, 1984; Ireland *et al.*, 1992). These values are thought to represent the mean isotopic composition of the dust component of the solar nebula (Clayton, 1993), with little or no exchange with nebular gas subsequent to the formation of the grains. In contrast, Simon *et al.* (1994) showed that large (50–300 μm) Mg-, Al-, Cr-spinel crystals and crystal fragments recovered from the products of freeze–thaw disaggregation of Murchison have near-normal O-isotopic compositions and exhibit a variety of zoning patterns with respect to Cr_2O_3 contents. Simon *et al.* (1994) termed the observed zoning patterns patchy, gradational, chevron, and core-rim, plus homogeneous (*i.e.*, unzoned). Patchy grains have numerous islands, typically 10–20 μm across, of contrasting Cr_2O_3 contents. In the gradational type, Cr_2O_3 abundance varies smoothly across the grains. Chevron-zoned grains have approximately 5–10 angular, sharply defined bands with differing Cr_2O_3 contents. Core-rim grains have low-Cr_2O_3 cores enclosed by high-Cr_2O_3 rims. These coarse grains are rarely found *in situ* in the meteorite, however, hindering our ability to make accurate petrologic interpretations.

In a survey of sawn surfaces of Allende specimens, we found coarse-grained Mg-, Al-, Cr-spinels with compositions and zoning patterns similar to those found in Murchison spinels. We have investigated the mineral chemistry, zoning, and O-isotopic compositions of a suite of spinel-bearing Allende chondrules and inclusions to determine how the spinel formed, whether it may be related to spinel in CAIs, and to compare it with the coarse spinel from Murchison. We also note the suggestion (*e.g.*, Steele, 1986) that isolated grains of blue-luminescing, near-endmember forsterite that are found in both CM2 and CV3 chondrites are from a single condensate population that was sampled by both of these meteorite groups. Here we consider whether there also might have been a population of condensate spinel grains that was sampled by both Allende and Murchison. Preliminary reports of these results were given by Simon *et al.* (1998, 1999).

ANALYTICAL METHODS

A chip of the Allende meteorite containing an inclusion with a huge (1 mm), red, single crystal of Cr-bearing spinel was sent to us by Mr. S. Kambach of Lörrach, Germany. This discovery inspired

us to undertake a search of our collection of sawn slabs of Allende for additional occurrences of red spinel, using a binocular microscope. Including the Kambach sample, a total of 17 polished thin sections were prepared, 13 of which contain Cr-spinel-bearing objects; a subset of these are discussed in detail here. We also studied thin sections of Red Eye, a large Cr-spinel-bearing Allende chondrule, from the Caltech collection. Samples were examined optically with a petrographic microscope. Backscattered electron images and digital x-ray maps were obtained with a JEOL JSM-5800 LV scanning electron microscope equipped with an Oxford/Link ISIS-300 energy dispersive microanalysis system. Quantitative wavelength dispersive x-ray analyses were obtained with a Cameca SX-50 electron microprobe operated at 15 kV. Data were reduced *via* the modified ZAF correction procedure PAP (Pouchou and Pichoir, 1984). We assumed that Fe is present as Fe^{2+}. This resulted in excellent stoichiometry and cation totals, which suggests that Fe^{3+} abundances are negligible.

Oxygen-isotopic abundances were determined with the UCLA Cameca IMS 1270 ion microprobe using techniques similar to those described by McKeegan *et al.* (1998). Measurements were made by sputtering polished, C-coated thin sections with a 12–20 μm diameter Cs^+ beam. Negative secondary ions with low initial kinetic energy (0 to ~30 eV) were analyzed at high-mass resolving power ($m/\Delta m$ > 6500) in order to separate interfering molecular species ($^{16}OH^-$, $^{17}OH^-$, $^{16}OH_2^-$) from atomic O ions; corrections for tailing of $^{16}OH^-$ into the $^{17}O^-$ peak were always <0.5‰, and typically <0.1‰, in $\delta^{17}O$. Charge compensation was achieved with the use of a normal-incidence electron gun. A Faraday cup detector was used to measure the intense $^{16}O^-$ current (60–80 × 10^6 ions/s equivalent), whereas $^{17}O^-$ and $^{18}O^-$ were measured by pulse counting with an electron multiplier. Ion intensities were corrected for background (Faraday cup) and deadtime (electron multiplier); both corrections can be made with high (~0.1‰) accuracy at these count rates.

The measured ion ratios were corrected for instrumental mass fractionation and relative detector efficiencies (electron multiplier/Faraday cup ratio) by comparison to measurements made on terrestrial O-isotopic standards, Burma spinel, and San Carlos olivine, interspersed with those of the unknowns. The reported (1σ) uncertainties include both the internal measurement precision on an individual analysis (typically ~1‰) summed quadratically with the standard deviation of the mean (in both $\delta^{18}O$ and $\delta^{17}O$) of measurements of the spinel standard during a given analysis session (typical values ranged from ~0.5 to 1.5‰). This procedure provides a reasonably conservative estimate of the overall uncertainty associated with the analysis of a single spot on the sample due to both statistical fluctuations and other random errors associated with the reproducibility of the ion microprobe analyses. Systematic errors in the instrumental mass fractionation correction, due to differences in the major element composition of the unknowns from that of the standard, could possibly lead to inaccuracies in the calculated isotopic composition of a sample relative to the SMOW scale. This is potentially a concern for some of the spinel samples analyzed here because of their variable chemical compositions, especially the elevated Cr_2O_3 and FeO contents relative to our Burma spinel ($MgAl_2O_4$) standard. However, under our analytical conditions (*i.e.*, low energy ions), such "matrix effects" are generally small between refractory oxide minerals. For example, measurements of a terrestrial spinel (Russell *et al.*, 1998) containing 19% FeO, when corrected for instrumental mass fractionation by the Burma spinel standard, yielded $\delta^{18}O$ = 4.25 ± 0.30‰, $\delta^{17}O$ = 2.02 ± 0.64‰ (corresponding to $\Delta^{17}O$ = –0.19 ± 0.29‰) compared to laser-fluorination analyses of $\delta^{18}O$ = 4.95, $\delta^{17}O$ = 2.58‰. Thus, in this case, any possible matrix effect is at most ~0.5‰ per amu. Similarly, analyses of San Carlos olivine, normalized by the Burma spinel standard, yield $\delta^{18}O$ = 3.61 ± 0.30‰, $\delta^{17}O$ = 2.01 ± 0.64‰ ($\Delta^{17}O$ = 0.13 ± 0.15‰), which implies a matrix effect of only ~0.8‰ per amu between spinel and olivine (Fo_{89}). Although we have not determined whether a matrix effect exists between Burma spinel and Cr-rich spinels, the small magnitude of such effects between a variety of refractory oxide and silicate minerals, including those that contain significant amounts of Fe, which is known to be an important factor in changing instrumental mass fractionation by secondary ion mass spectrometry (*e.g.*, Eiler *et al.*, 1997), indicates that inaccuracies produced by these potential artifacts are likely to be at most approximately 1–2‰ per amu. Because this is comparable to the analytical precision, we have not included an additional uncertainty due to possible matrix effects. Note that, because they only affect the magnitude of the correction of instrumental mass fractionation, matrix effects have no influence on the determination of $\Delta^{17}O$, the deviation from the terrestrial mass fractionation line.

RESULTS

Petrography of Chromium-Spinel-bearing Objects

With the exception of Red Eye, the Allende samples considered here were given the prefix ALSP for (Al)lende (sp)inel and numbered ALSP1–ALSP17. A spinel-bearing object has the same number as its host thin section unless more than one object was found in the same section. In that case, the objects are distinguished by the addition of A and B to the number, as in ALSP11A and ALSP11B. Characteristics of the spinels are summarized in Table 1. Because

TABLE 1. Summary of characteristics of spinel-bearing objects.

Sample no.	Object type*	Spinel zoning type†	Cr_2O_3 range (wt%)	FeO range (wt%)
ALSP1	ORO	Chevron	0.74–8.5	0.49–16.1
ALSP2A	BO	Patchy; Homog.	6–19; 37	12–17; 32
ALSP2B	PO	Patchy	9.4–31.0	17.4–31.0
ALSP3	PO	Homogeneous	48	36
ALSP4	GO	Patchy	6.4–13.8	4.3–9.7
ALSP5A	ORO	Homogeneous	34	25
ALSP5B	ORO	Homogeneous	46	36
ALSP8	BO	Patchy	23.9–31.1	5.8–17.5
ALSP10	CCH	Patchy	31.0–44.2	12.8–28.8
ALSP11A	ORO	Homogeneous	36 (FG); 50 (CG)‡	38 (FG); 23 (CG)
ALSP11B	BO	Patchy	12–30	11–23
ALSP12	BO	Patchy	9–17	8–18
ALSP13	CCH	Gradational	4.1–13.6	2.2–5.4
ALSP14A	PO	Patchy	7.9–20.9	2.7–23.2
ALSP16	BO	Patchy	18–40	17.5–30
ALSP17	BO	Gradational	3.5–17	2–3
Red Eye	PO	Patchy; Grad.; Homogeneous	17.3–38.7; 20.9–40.5; 25	4.0–15.1; 5.0–15.1; 8

*ORO = olivine-rich object; BO = barred olivine chondrule; PO = porphyritic olivine chondrule; GO = granular olivine chondrule; CCH = compound chondrule.
†After Simon *et al.* (1994).
‡FG = fine-grained; CG = coarse-grained.

coarse igneous rock fragments have never been observed in carbonaceous chondrites, we equate an igneous texture with a chondrule source. Most of the spinels we found occur in chondrules or chondrule fragments, with barred and porphyritic textures being the most commonly represented types. Some host objects could not be unambiguously identified as chondrules (*i.e.*, as having formed from liquid droplets), and these are termed "olivine-rich objects" in Table 1. The occurrence of patchy spinels in chondrules is somewhat surprising given the conclusion of Simon *et al.* (1994), in the absence of paragenetic relations, that these spinels are sintered aggregates that were probably never molten.

The spinel in ALSP1 appeared deep red in the sawn slab and is pale pink in transmitted light. A backscattered electron image (Fig. 1a) shows that the spinel grain, approximately 1 × 0.75 mm, is a fragment of a once-larger crystal and has several straight bands of contrasting electron albedo that define the chevron zoning (Simon *et al.*, 1994) of the grain. These layers are truncated at the broken left edge (as shown in Fig. 1a) of the crystal and along the other irregular edges of the grain. Comparison with a Cr x-ray map (Fig. 1b) shows that backscattered electron albedo variations within the spinel crystal are closely correlated with Cr contents. The outer layers of the spinel crystal contain rounded inclusions of aluminous diopside that are ~30 μm across and are associated with voids in the spinel. Many of the spinel grains separated from Murchison have similar inclusions and voids (Fig. 1 of Simon *et al.*, 1994). The spinel in ALSP1 is almost completely enclosed by an assemblage of anhedral to subhedral, 50–100 μm grains of forsterite (Fo_{95-99}) set in a fine-grained groundmass of nepheline and relatively Fe-rich olivine (Fo_{59-85}). The coarse olivine grains have cores that exhibit the blue cathodoluminescence that is typical of forsterite enriched in refractory elements (*e.g.*, Steele, 1986), and Fe-rich (Fo_{62-73}) rims and veins that are common in olivine in oxidized CV3 chondrites (*e.g.*, Weinbruch *et al.*, 1990).

Red Eye (Fig. 1c) is a large coarse-grained chondrule consisting mainly of olivine but also containing coarse (>150 μm), subhedral to anhedral, Cr-bearing spinel grains and minor pyroxene and plagioclase. The chondrule is dominated by one anhedral olivine grain that is approximately 4 × 3 mm. The spinel, pyroxene, and plagioclase mainly occur intergrown in a band ~500 μm from the chondrule rim.

Sample ALSP4 (Fig. 1d) is a 750 × 500 μm chondrule fragment consisting of subhedral olivine grains that are 50–100 μm across with interstitial Cr-, Al-spinel (three grains, approximately 50–75 μm), aluminous diopside (two grains, ~200 μm), and a groundmass of clinopyroxene, plagioclase, and nepheline.

After ALSP1, the largest spinel we found is that in ALSP11A, a 320 × 280 μm fragment (Fig. 1e) dominated by a deep red, rectangular spinel grain that is 150 × 110 μm. Along a broken edge of the fragment, the spinel is in contact with the meteorite matrix. Otherwise, it is enclosed by subhedral olivine grains 5–90 μm across. Many of these olivines contain fine (~5 μm) spinel grains near their rims. Interstitial pentlandite grains, ≤5 μm across, are also present. An unusual feature of this object is that there is much pore space between some olivine grains, giving the object a spongy texture, and making us reluctant to classify it as a chondrule. As shown in Fig. 1f, some cavities are lined with euhedral olivine, reminiscent of vapor-deposited crystals found in cavities in some refractory inclusions (*e.g.*, Allen *et al.*, 1978).

Sample ALSP14A (Fig. 1g) is a 700 × 500 μm chondrule fragment dominated by a 400 × 400 μm, embayed olivine grain in a mesostasis of herringbone-textured clinopyroxene with interstitial olivine and feldspathoids. No spinel is present in the mesostasis, but in the largest olivine embayments sit ragged grains of pink spinel that are 50–100 μm across. One of these grains is shown in Fig. 1h. The irregular shape and patchy zoning are quite evident in this image.

Mineral Chemistry and Zoning

Spinel–Representative analyses of spinel are given in Table 2. The backscattered electron image of ALSP1 (Fig. 1a) shows several

TABLE 2. Representative electron microprobe analyses of spinel.

	ALSP1		RED EYE		ALSP11A	ALSP14A	
	1	2	1	2	1	1	2
MgO	27.65	25.11	20.47	16.40	8.60	24.52	15.25
Al_2O_3	70.97	61.79	44.99	30.93	16.57	56.44	49.00
SiO_2	0.03	0.07	0.09	0.12	0.02	0.04	0.04
CaO	0.02	BDL	0.10	0.21	BDL	0.03	0.05
TiO_2	0.06	0.23	0.36	0.81	0.65	0.28	0.26
V_2O_3	0.10	0.37	0.38	0.63	0.58	0.32	0.35
Cr_2O_3	0.96	8.49	24.56	38.17	50.29	14.45	18.25
FeO	0.55	3.64	8.20	12.64	23.33	3.82	16.86
Total	100.34	99.70	99.15	99.91	100.04	99.90	100.06
			Cations per four O anions				
Mg	0.978	0.931	0.828	0.712	0.417	0.928	0.622
Al	1.985	1.813	1.440	1.062	0.635	1.689	1.582
Si	0.001	0.002	0.003	0.003	0.001	0.001	0.001
Ca	0	0	0.003	0.006	0	0.001	0.001
Ti	0.001	0.004	0.007	0.018	0.016	0.005	0.005
V	0.002	0.007	0.008	0.015	0.015	0.007	0.008
Cr	0.018	0.167	0.527	0.879	1.293	0.290	0.395
Fe	0.011	0.076	0.186	0.308	0.635	0.081	0.386
Total cations	2.996	3.000	3.002	3.003	3.012	3.002	3.000

BDL = below detection limit of the electron microprobe of 0.013 wt%. Data were reduced with all Fe as Fe^{2+}; excellent stoichiometry and cation totals suggest that Fe^{3+} abundances are negligible.

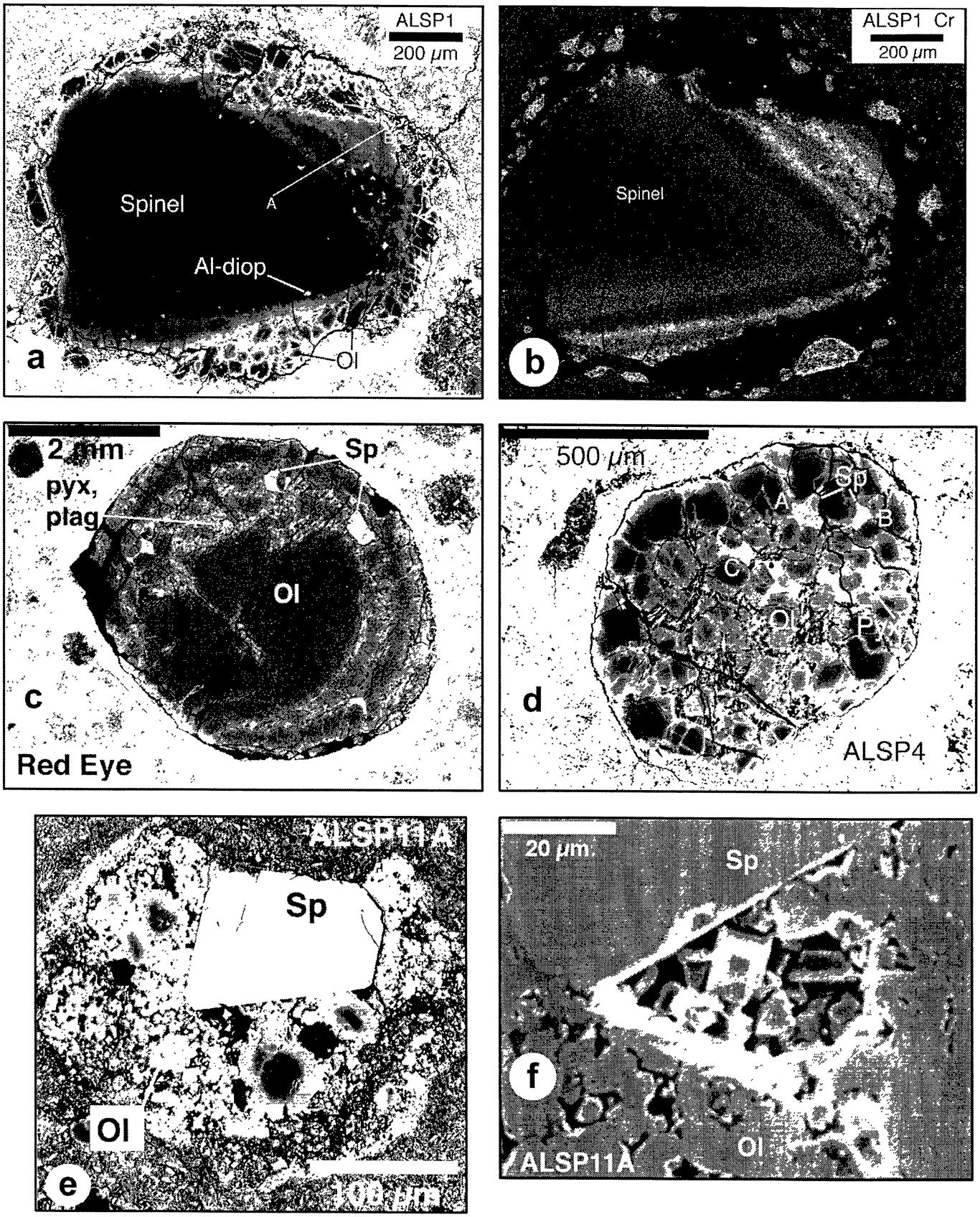

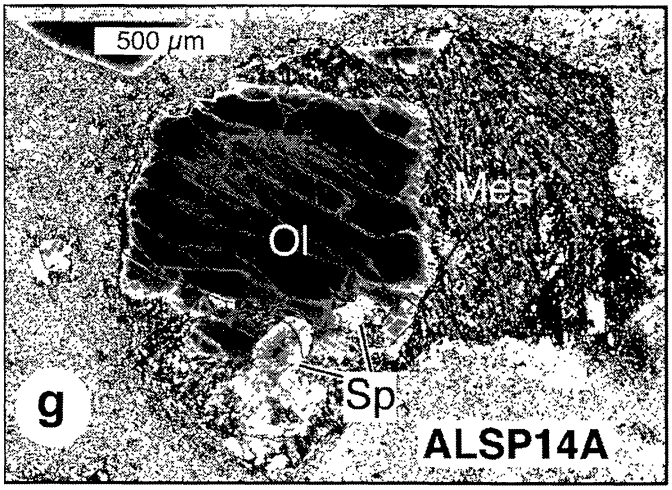

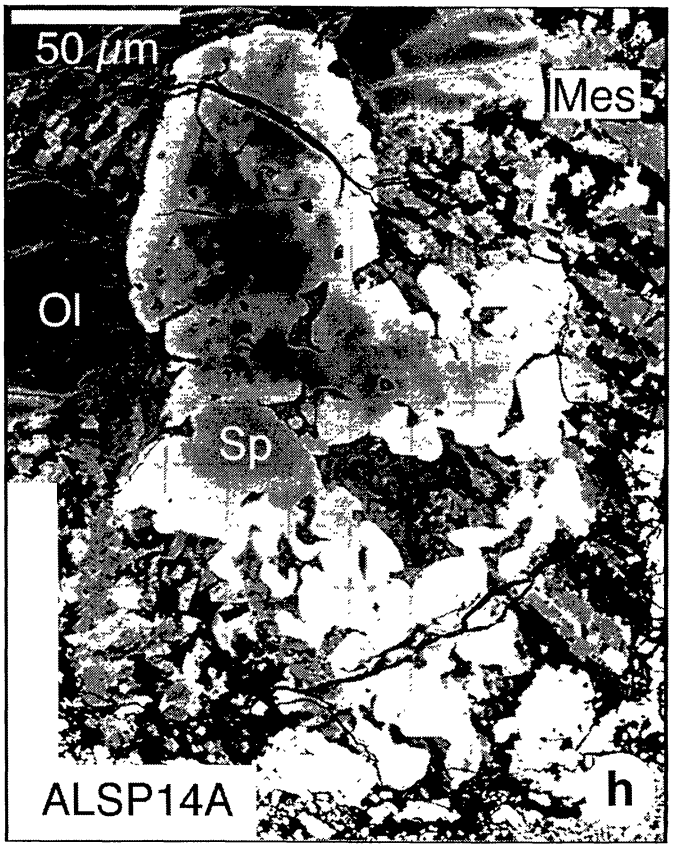

FIG. 1. (left and above) Images of spinel-bearing objects in Allende. (a) Backscattered electron photomosaic of ALSP1. Note truncation of straight zoning bands, which suggests that the crystal was once larger. Note also the bright, FeO-rich rims enclosing most olivine (Ol) grains. Al-diop = aluminous diopside. Location of electron microprobe traverse along path *A–B* is also indicated. (b) Chromium x-ray map of ALSP1, clearly showing chevron zoning with respect to Cr contents of the spinel. (c) Backscattered electron image of Red Eye, a large olivine-rich chondrule. Sp = spinel. Pyroxene (pyx) and plagioclase (plag) crystallized late and are concentrated in the light gray band around the central olivine crystal. (d) Backscattered electron image of chondrule ALSP4. Spinel grains A, B, and C are indicated. Groundmass, seen mostly near the center of the chondrule, consists of pyroxene, plagioclase, and nepheline. (e) Backscattered electron image of ALSP11A, which has a large, Cr-, Fe-rich spinel. Note Mg-rich (dark) cores of some olivine grains and void space (black) between grains. Small, bright grains enclosed in olivine are Cr-, Fe-rich spinel and pentlandite. (f) Secondary electron image of ALSP11A showing euhedral olivine crystals in a pocket adjacent to the large spinel (upper left). (g) Backscattered electron image of ALSP14A, a chondrule fragment with coarse, corroded olivine and spinel in a mesostasis (Mes) of herringbone-textured pyroxene with minor olivine and feldspathoid. (h) Backscattered electron image of patchy spinel in ALSP14A.

straight layers of contrasting electron albedo. Comparison of that image with a Cr x-ray map of the object (Fig. 1b) shows a strong correlation between the layering and Cr abundance. The results of an electron probe traverse across several layers, along the path *A–B* shown in Fig. 1a, are summarized in Fig. 2a. They show that Cr_2O_3 contents fluctuate, decreasing from approximately 2.5 wt% in the interior to <2 wt% in a Cr-poor layer, then increasing and decreasing several times, reaching ~8.5 wt% in the most Cr-rich layer. Abundances of Al_2O_3 are so strongly anticorrelated with those of Cr_2O_3 that a plot of Al_2O_3 data for this traverse would be the complement of the Cr_2O_3 trend. This observation, along with excellent stoichiometry of the electron probe analyses, which were reduced assuming all Fe as FeO, indicates that Al, and not Fe^{3+}, is substituting for Cr. The FeO contents are uniformly ~0.5 wt% in the interior of the grain and increase toward the rim of the grain, reaching 13 wt% at the edge. There is a strong anticorrelation between FeO and MgO, and, as Fig. 2a shows, no correlation between FeO and Cr_2O_3. A lack of correlation between FeO and Cr_2O_3 was also observed in many of the spinels separated from Murchison (Simon *et al.*, 1994).

Another similarity between the spinel in ALSP1 and chevron-zoned spinel in Murchison can be seen in Fig. 2b, a plot of V_2O_3 *vs.* TiO_2. Two of the Murchison grains have relatively low V_2O_3 contents, but otherwise there is a high degree of overlap between the data sets.

Of the six spinel grains present in the Red Eye sections, three have patchy zoning, two are homogeneous, and one has gradational zoning. At spinel–plagioclase contacts, 10–20 μm thick bands of relatively chromite-rich spinel grains occur. Chondrules ALSP14A and ALSP4 also contain patchy spinel. The coarse spinel grain in ALSP11A is homogeneous, except for a thin (~10 μm), relatively FeO-rich rim. The interior of the spinel has ~50 wt% Cr_2O_3 and ~23 wt% FeO, the rim ~48 and 30 wt%, respectively. The fine-grained spinel has less Cr_2O_3 and more FeO, with 36 and 38 wt%, respectively, than the coarse grain. In both Red Eye and ALSP11A, the homogeneous grains are free of inclusions, as is the case among homogeneous Murchison spinels (Simon *et al.*, 1994).

In contrast with the spinel in ALSP1, FeO is positively correlated with Cr_2O_3 in Red Eye and ALSP14A spinel. The spinel in ALSP4 is unusual. Figure 3 shows electron probe data for three grains, A, B, and C. In grain A, FeO and Cr_2O_3 are positively correlated, and in the other two they are not. In grain B, Cr_2O_3 varies only between 9 and 10.5 wt% whereas FeO ranges from 4.5 up to ~8 wt%. In grain C, both FeO and Cr_2O_3 vary widely. In all three grains, FeO contents increase from core to rim; but in grains B and C, the Cr_2O_3 contents do not, resulting in the contrasting Fe-Cr trends seen in Fig. 3. Red Eye and ALSP4 show that even within a single chondrule, spinel can exhibit a variety of compositions and zoning styles.

The contents of V_2O_3, TiO_2, and Cr_2O_3 in the patchy spinel in these chondrules are compared to those of patchy spinel in other Allende chondrules from our suite (Table 1) and to patchy spinel from Murchison in Fig. 4. The results show that there is a

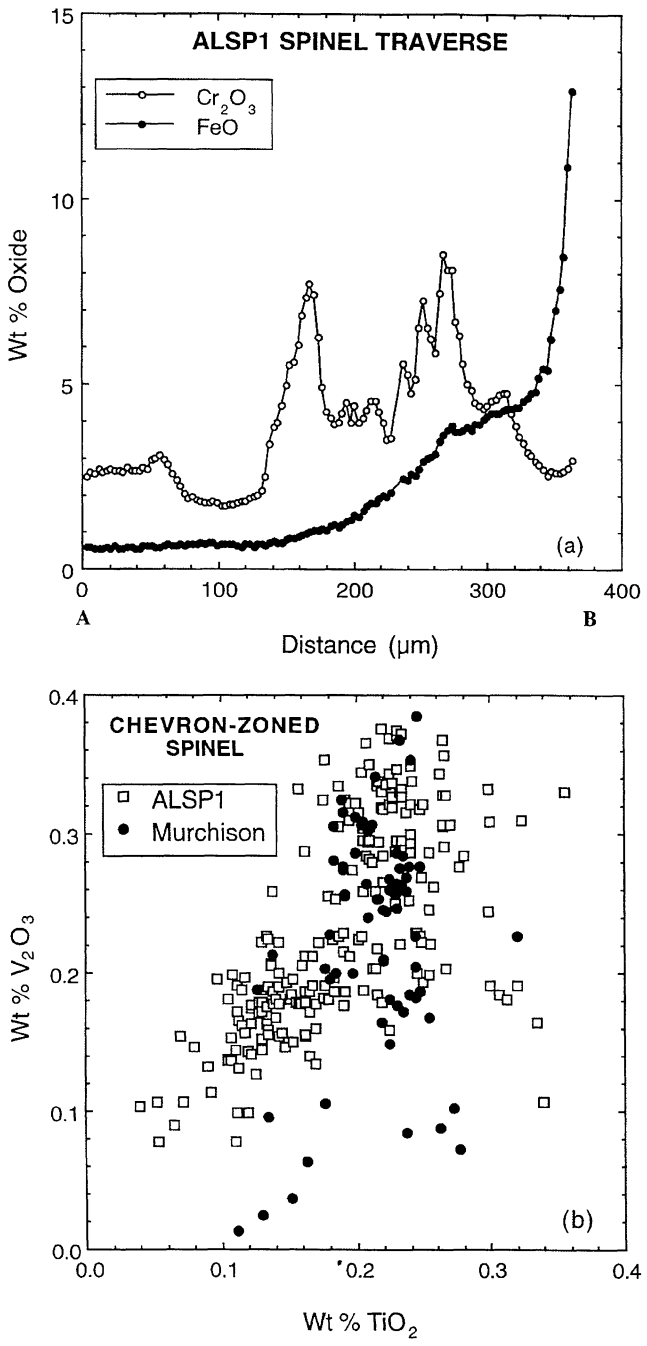

FIG. 2. Electron probe analyses of spinel. (a) Abundances of Cr_2O_3 and FeO as a function of distance along path *A–B* in ALSP1 (Fig. 1a). The Cr_2O_3 contents vary as bands are crossed whereas FeO contents increase with decreasing distance from the rim (at *B*). (b) Comparison of analyses of ALSP1 with those of chevron-zoned spinel from Murchison. Note the high degree of overlap between the data sets.

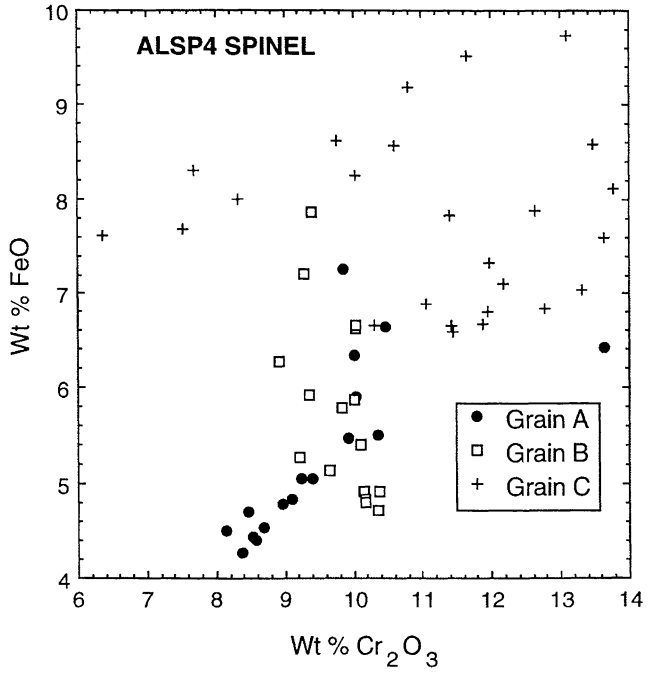

FIG. 3. Analyses of spinel in chondrule ALSP4. The three grains analyzed exhibit three different Fe-Cr relationships. Contents of FeO increase from core to rim within each grain, but those of Cr_2O_3 do not.

significant degree of overlap between the Allende and Murchison samples, and the data plot along the same general trends. The Murchison compositions extend to very low Cr_2O_3 contents, however, whereas the Allende analyses range to fairly high Cr_2O_3 (>25 wt%) contents. This may reflect, at least in part, a sampling bias. The relatively faint color of low-Cr_2O_3 spinel is probably easier to detect against the white background of the Murchison picking dish than in the Allende slab surfaces, so low-Cr_2O_3 spinel might be underrepresented in the present Allende suite.

Olivine–The coarse olivine in ALSP1 is very Mg-rich, Fo_{95-99}. The cores of the grains have ~0.6 wt% CaO, 0.5 wt% FeO, and 0.2–0.4 wt% Al_2O_3. The abundances of CaO and Al_2O_3 decrease toward the rims of the grains (*i.e.*, with increasing FeO). Most of the grains have relatively FeO-rich (Fo_{62-73}) veins and rims, which are typical of olivine in oxidized CV3 chondrites (Weinbruch *et al.*, 1990). Representative analyses of olivine in this and in other samples are given in Table 3.

Olivine has narrow composition ranges in chondrules Red Eye (Fo_{92-95}) and ALSP4 (Fo_{93-97}). Most of the olivine in ALSP11A is Fe-rich, with compositions between Fo_{47} and Fo_{55}. Several of the larger grains have magnesian cores (Fo_{83-88}) and ferroan rims in a textural relationship reminiscent of relic forsteritic olivine found in some chondrules (*e.g.*, Jones, 1992). These rims in ALSP11A are thicker than those in ALSP1. In ALSP14A, the coarse olivine grain is zoned, with FeO contents increasing inward (to Fo_{88}) and outward (to Fo_{86}) from a ring of nearly pure forsterite (Fo_{99}). Fine-grained olivine in the mesostasis has a wide range of compositions, from ~Fo_{60} to ~Fo_{85}.

One way to compare olivine compositions is on a plot of Cr_2O_3 *vs.* FeO (Fig. 5). Isolated grains from CV meteorites tend to have low Cr_2O_3 contents over a wide range of FeO contents, whereas most olivine compositions from CM meteorites fall on a trend that has a wide range of Cr_2O_3 contents over a narrow range of FeO contents (Steele and Smith, 1986; Steele, 1992). As shown in Fig. 5, analyses of olivine in the spinel-bearing objects ALSP1 and ALSP11A and in the chondrule fragment ALSP14A generally follow the CV trend. With one exception in each sample, the ALSP11A and ALSP14A analyses with >0.3 wt% Cr_2O_3 are within ~10 μm of spinel. In contrast, compositions of olivine in chondrules ALSP4 and Red Eye define vertical trends on Fig. 5, with Cr_2O_3

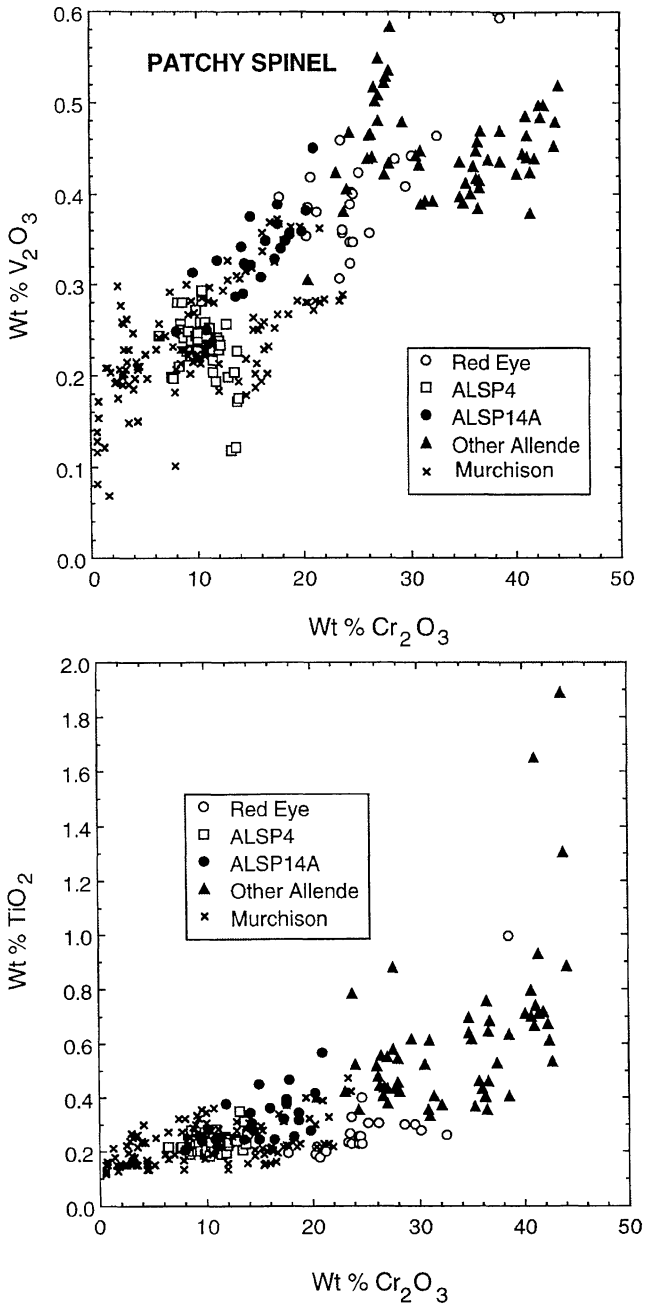

FIG. 4. Compositions of patchy spinel in Allende chondrules compared to those recovered from Murchison. The data from the two meteorites plot on the same trends as each other. "Other Allende" refers to samples listed on Table 1 but are not described in detail in this report.

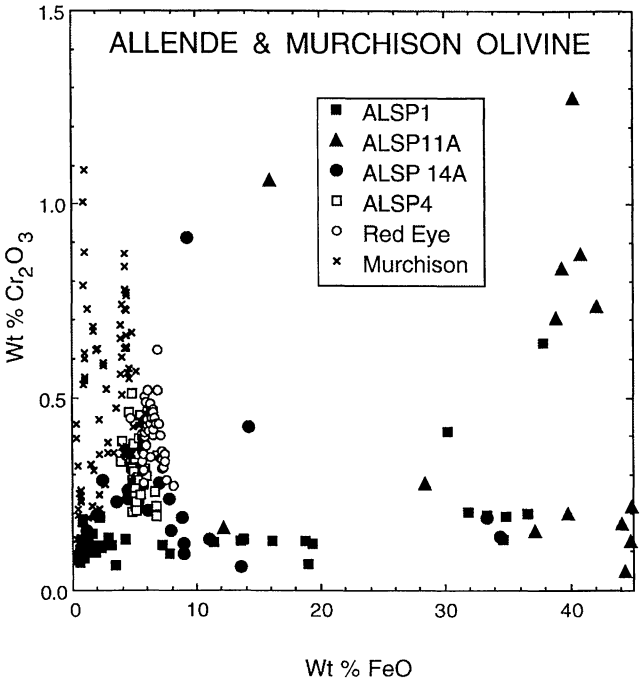

FIG. 5. Compositions of olivine in Cr-spinel-bearing objects in Allende and Murchison. Data from ALSP1, ALSP11A, and ALSP14A follow a low-Cr_2O_3, CV-like trend, whereas those from ALSP4 and Red Eye follow a near-vertical, CM-like trend (Steele and Smith, 1986), typical of Murchison.

contents ranging from approximately 0.2–0.6 wt%, reminiscent of the CM trend. Analyses of olivine from spinel-bearing objects in Murchison, both in thin sections of the meteorite and recovered from freeze–thaw separates, are plotted for comparison in Fig. 5 and define a near-vertical trend, like that seen for isolated grains in Murchison (Steele and Smith, 1986), at lower FeO contents than those of the Allende chondrules.

Pyroxene–Representative analyses are given in Table 4. The spinel in ALSP1 contains small inclusions of aluminous diopside, as do many spinel grains separated from Murchison (Simon *et al.*, 1994). Figure 6 shows that the pyroxene in ALSP1 is similar in composition to much of the pyroxene in the Murchison samples, with overlapping Al_2O_3, SiO_2, Cr_2O_3, and TiO_2 contents. Pyroxene from the other Allende objects tends to be less aluminous and contains more Cr_2O_3 than those from ALSP1 and Murchison.

Oxygen-Isotopic Compositions

The O-isotopic compositions measured in individual phases in the inclusions considered here are given in Table 5 and illustrated in Fig. 7. Oxygen-isotopic compositions of spinels separated from Murchison (Simon *et al.*, 1994) are shown in Fig. 7f for comparison with the present work. The analyses of ALSP1 (Fig. 7a) spinel plot just below the terrestrial fractionation line and within the range of the Murchison analyses. The analysis spots in ALSP1 traverse chemical zoning bands that have from 1 to 6 wt% Cr_2O_3, but the O-isotopic ratios are fairly homogeneous. They are quite distinct, however, from the compositions of adjacent olivine, which are much more ^{16}O-rich. As Fig. 7a shows, the olivine analyses plot on the mixing line defined by analyses of whole Allende CAIs (Clayton *et al.*, 1977). Their O-isotopic ratios are similar to those reported for refractory forsterite grains, both isolated and in chondrules, in Allende (Weinbruch *et al.*, 1993; Leshin *et al.*, 1998).

In ALSP11A (Fig. 7b), the spinel analyses are from the interior of the grain and they show that it is isotopically homogeneous in addition to being chemically uniform. Its composition, with $\delta^{18}O = -1.3 \pm 1.8‰$ and $\delta^{17}O = -4.4 \pm 2.0‰$, is slightly more ^{16}O-rich than most of the other spinels analyzed and plots well within error of the CAI line, making it unique among Cr-bearing spinel. The Mg-rich cores of the enclosing olivine grains are also somewhat ^{16}O-rich relative to their FeO-enriched rims. In fact, the spinel and the forsteritic olivine in ALSP11A have the same O-isotopic compositions (which plot on the CAI line), which argues against a significant

TABLE 3. Representative electron microprobe analyses of olivine in spinel-bearing objects and chondrules.

	ALSP1, coarse ol.	ALSP1, coarse ol.	In mesostasis	Red Eye	ALSP4	ALSP11A	ALSP14A
MgO	57.52	56.47	30.59	52.12	52.92	27.82	50.53
Al_2O_3	0.25	0.40	0.24	0.10	0.21	0.02	0.04
SiO_2	42.37	41.77	36.19	41.94	42.20	34.93	40.65
CaO	0.66	0.56	0.07	0.18	0.60	0.42	0.38
Cr_2O_3	0.10	0.09	0.19	0.43	0.34	0.15	0.12
TiO_2	0.11	0.11	0.05	BDL	0.09	BDL	0.04
MnO	0.03	0.01	0.17	NA	NA	0.22	0.07
FeO	0.52	0.76	33.35	6.36	4.95	37.12	8.96
Total	101.56	100.17	100.85	101.13	101.31	100.68	100.79
			Cations per four O anions				
Mg	1.989	1.981	1.242	1.852	1.867	1.158	1.827
Al	0.007	0.011	0.008	0.003	0.006	0	0.001
Si	0.983	0.983	0.986	1.000	0.999	0.976	0.987
Ca	0.016	0.014	0.002	0.005	0.015	0.013	0.010
Cr	0.002	0.002	0.004	0.008	0.006	0.003	0.002
Ti	0.002	0.015	0.001	0	0.002	0	0.001
Mn	0.001	0	0.004	–	–	0.005	0.001
Fe	0.010	0.015	0.760	0.127	0.098	0.867	0.182
Total	3.010	3.021	3.007	2.955	2.993	3.022	3.011
Fo mol%	99.5	99.2	62.0	93.6	95.0	57.2	90.9

BDL = below detection limit of electron probe of 0.043 wt%. NA = not analyzed.

TABLE 4. Representative electron microprobe analyses of pyroxene in spinel-bearing objects.

	ALSP1	ALSP1	Red Eye	Red Eye	ALSP4	ALSP11A	ALSP14A
MgO	14.30	18.16	30.76	19.02	15.93	12.14	19.06
Al_2O_3	14.21	13.24	2.00	4.23	9.91	4.68	5.51
SiO_2	45.43	46.85	55.53	51.42	48.57	48.27	51.08
CaO	24.82	20.43	4.17	19.43	22.75	22.64	19.37
Cr_2O_3	0.27	0.44	1.28	1.55	1.39	1.45	1.76
TiO_2	1.03	1.27	0.58	1.16	1.29	1.40	1.86
V_2O_3	BDL	BDL	0.07	0.12	0.06	0.08	NA
FeO	0.29	0.19	6.32	3.14	0.92	8.74	2.07
Total	100.35	100.58	100.71	100.07	100.82	99.40	100.71
			Cations per four O anions				
Si	1.642	1.667	1.930	1.860	1.743	1.828	1.827
^{IV}Al	0.358	0.333	0.070	0.140	0.257	0.172	0.173
^{VI}Al	0.247	0.222	0.011	0.041	0.162	0.037	0.059
Mg	0.770	0.963	1.593	1.026	0.852	0.685	1.016
Ca	0.961	0.779	0.155	0.753	0.875	0.919	0.742
Cr	0.008	0.012	0.035	0.044	0.039	0.044	0.050
Ti	0.028	0.034	0.015	0.031	0.035	0.040	0.050
V	0	0	0.002	0.004	0.002	0.002	–
Fe	0.009	0.006	0.184	0.095	0.028	0.277	0.062
Total oct.	2.023	2.016	1.995	1.994	1.993	2.004	1.979

BDL = below detection limit of electron probe of 0.027 wt%. NA = not analyzed.

matrix effect due to the high Cr-content of the spinel. Unfortunately, the Fe-enriched rim of the spinel grain is too narrow for isotopic analysis.

In contrast, in chondrules ALSP4, ALSP14A, and Red Eye (Fig. 7c–e, respectively), spinel and coexisting silicates (olivine and clinopyroxene) are in apparent isotopic equilibrium. In ALSP14A, although the olivine and spinel appear to be corroded (Fig. 1g) and therefore out of equilibrium with their host, their O-isotopic compositions are quite similar to that of the pyroxene-rich mesostasis, as shown in Fig. 7d. In all three cases, within a given chondrule, analyses of different phases are within error of each other and are similar to analyses of whole Allende chondrules (Clayton *et al.*, 1983).

DISCUSSION

Formation of ALSP1

Using our petrographic observations, electron probe, and ion probe results, we can construct a model for the formation of ALSP1. Although it superficially may appear similar to a chondrule fragment, it is highly unlikely that ALSP1 formed by crystallization of a molten spherule. We equate an igneous origin with a chondrule source, so for ALSP1 to have crystallized from a liquid would

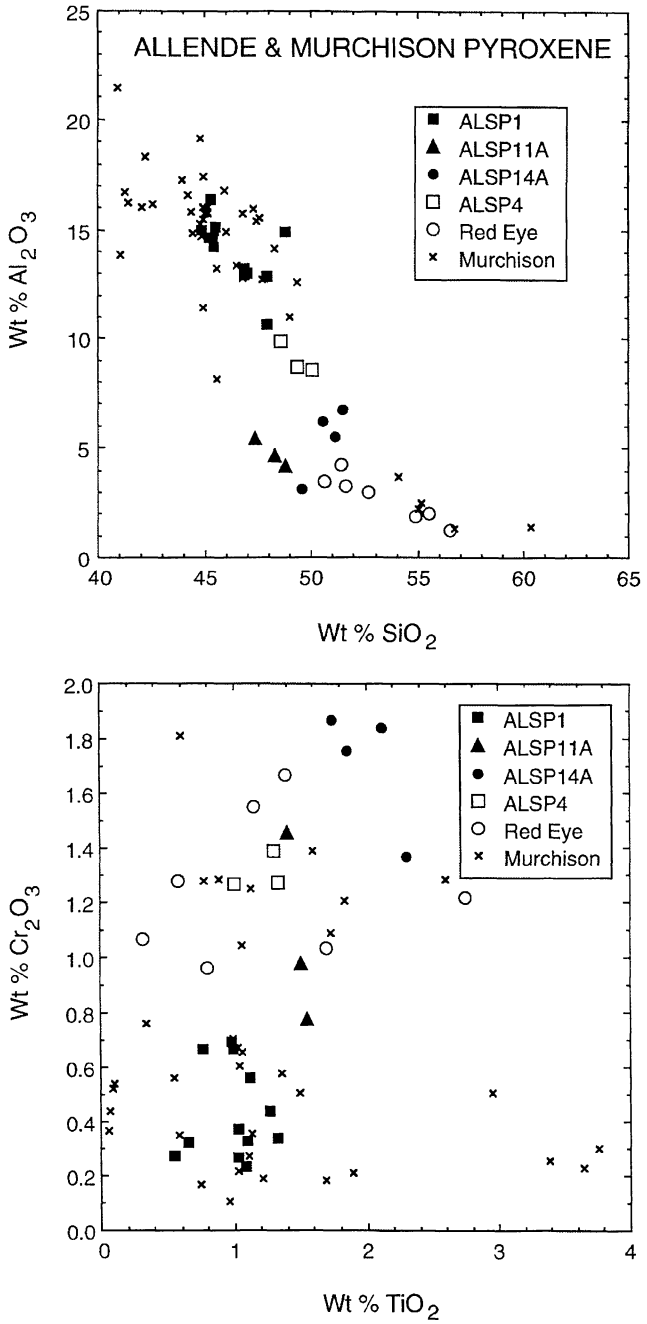

FIG. 6. Compositions of pyroxene in Cr-spinel-bearing objects in Allende and Murchison. The aluminous diopside found in ALSP1 is quite similar to that found enclosed in Murchison spinels.

TABLE 5. Oxygen-isotopic compositions of phases in Allende spinel-bearing objects (‰ relative to SMOW).*

Sample	Phase	$\delta^{18}O$	$\delta^{17}O$
	sp	−2.6 ± 1.4	−2.6 ± 1.1
	sp	−1.2 ± 1.3	−1.7 ± 1.1
	sp	0.4 ± 1.4	−0.8 ± 1.1
ALSP1	sp	0.0 ± 1.5	0.0 ± 1.3
	sp	0.8 ± 1.4	−0.8 ± 1.1
	sp	1.1 ± 1.4	−1.2 ± 1.1
	sp	−2.7 ± 1.4	−3.3 ± 1.2
	sp	−2.5 ± 1.4	−2.1 ± 1.1
	ol	−7.0 ± 1.4	−10.9 ± 1.2
	ol	−10.1 ± 1.4	−12.0 ± 1.1
	sp	2.0 ± 0.9	−0.6 ± 0.9
	sp	1.8 ± 0.9	−0.8 ± 0.9
	sp	1.7 ± 1.0	0.4 ± 0.9
	sp	2.4 ± 1.0	−1.6 ± 0.8
ALSP4	sp	1.1 ± 1.1	−2.1 ± 0.9
	sp	1.2 ± 1.0	−1.1 ± 1.1
	ol	5.8 ± 1.1	1.6 ± 0.9
	ol	2.4 ± 0.9	−1.2 ± 0.8
	ol	6.1 ± 0.9	0.7 ± 0.8
	pyx	5.1 ± 1.0	1.6 ± 1.2
	sp	−1.5 ± 1.8	−4.3 ± 2.0
	sp	−1.2 ± 1.7	−4.4 ± 1.9
ALSP11A	ol	2.5 ± 1.7	−3.4 ± 1.9
	ol	11.5 ± 1.8	3.6 ± 2.0
	ol	−0.2 ± 1.7	−5.3 ± 2.0
	sp	−4.2 ± 2.7	−5.9 ± 2.5
	sp	−1.1 ± 2.7	−2.1 ± 2.5
ALSP14A	ol	−0.2 ± 2.8	−2.6 ± 2.5
	ol	−0.6 ± 2.7	−3.4 ± 2.5
	pyx	−0.9 ± 2.7	−4.2 ± 2.4
	sp	0.9 ± 1.8	−0.2 ± 1.9
	sp	2.7 ± 1.8	0.7 ± 2.0
	sp	5.0 ± 1.9	2.6 ± 1.9
	sp	2.7 ± 1.9	2.0 ± 2.0
Red Eye	sp	3.7 ± 1.7	1.0 ± 1.9
	sp	2.5 ± 1.9	0.5 ± 2.0
	sp	1.6 ± 2.0	−0.9 ± 2.0
	ol	2.7 ± 1.9	0.7 ± 2.0
	ol	2.7 ± 2.0	1.9 ± 2.1
	ol	7.2 ± 1.7	3.2 ± 1.9

*Uncertainties are 1σ.
Abbreviations: sp = spinel; ol = olivine; pyx = pyroxene.

require a very unusual, Al-rich, Si-poor melt that not only crystallized spinel early, but did so in the form of a single, oscillatory-zoned grain. For the spinel in ALSP1 to be from a chondrule at all is unlikely, because (a) it is a crystal *fragment*, with one smooth broken edge and two rough irregular edges that are indicative of corrosion. The grain was therefore once somewhat larger, yet it is still ~1 mm across, so a parent chondrule would have had either an unusually spinel-rich composition or a size among the largest ever seen for a chondrule; (b) the development of oscillatory zoning in a grain within a chondrule would imply multiple fluctuations of conditions (*e.g.*, melt composition, temperature, O fugacity), which seem improbable to achieve in the short time frame during which chondrules are thought to have been molten; and (c) the grain would have to have been extracted from the chondrule and incorporated into its present host without any accompanying phases. The contrasting O-isotopic compositions of the spinel and olivine in ALSP1 (Fig. 7a) convincingly show that these two phases have different sources.

Although it seems unlikely that the spinel grain in ALSP1 formed by crystallization from a melt, this spinel is also too Cr- and Fe-rich to have condensed from a solar gas (Yoneda and Grossman, 1995). Spinel rich in Cr can, however, condense at equilibrium from a gas more oxidizing than solar. Ebel and Grossman (2000) have investigated the condensation of phases from systems made more oxidizing than a solar gas by the addition of dust having the

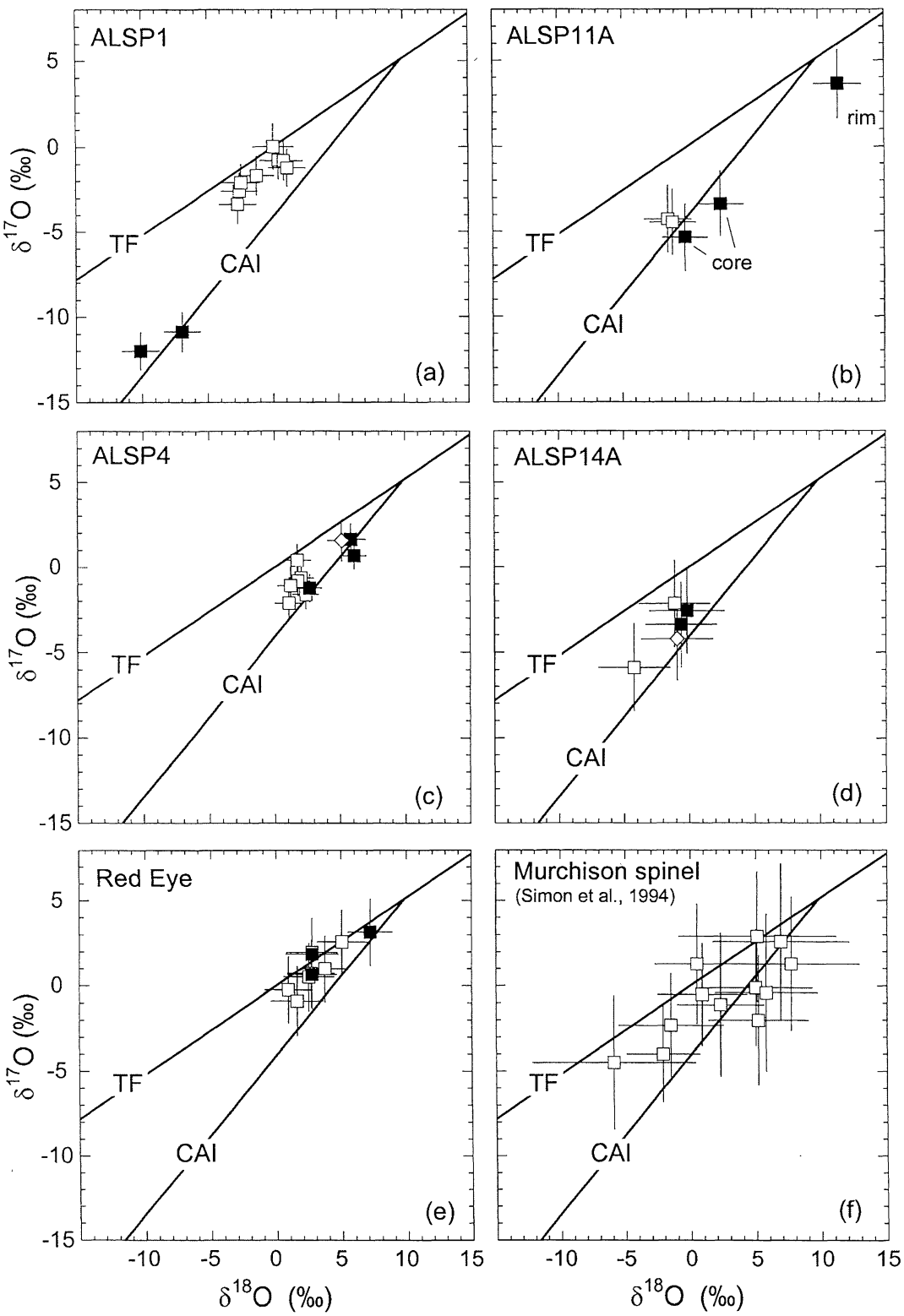

FIG. 7. Oxygen-isotopic compositions of individual phases in spinel-bearing objects. Open squares are spinel; filled squares are olivine; open diamonds are pyroxene; all uncertainties are 1σ. (a) ALSP1. Note the difference in isotopic composition between the spinel and the olivine in this sample. (b) ALSP11A. Spinel and magnesian olivine ("core") plot on the CAI line and are ^{16}O-rich, but the Fe-rich olivine ("rim") is relatively ^{16}O-poor. (c) ALSP4. All phases have similar, normal compositions. (d) ALSP14A. Compositions are homogeneous despite the corroded appearance of the olivine and spinel. (e) Red Eye. All compositions are normal. (f) Separated spinel from Murchison. Note the similarity of the compositions to those of Allende spinel. TF = terrestrial fractionation line. CAI = mixing line defined by analyses of whole Allende calcium-aluminum-rich inclusions (Clayton *et al.*, 1977).

composition of CI chondrites. Relatively oxidizing conditions stabilize Cr in spinel, and the amount of Cr_2O_3 that can enter spinel increases with decreasing temperature during condensation, which would be consistent with the general trend of increasing Cr_2O_3 contents from core to rim in the ALSP1 spinel. At a P^{tot} of 10^{-3} bar, a dust/gas enrichment of 100 relative to solar and a temperature of 1780 K, condensate spinel coexists with forsterite and FeO-free silicate liquid and has 2.4 wt% Cr_2O_3 and 0.2 wt% FeO. The contents of these oxides increase with decreasing temperature, reaching 6.1 and 0.4 wt% Cr_2O_3 and FeO, respectively, at 1720 K. This spinel dissolves into the silicate liquid by 1710 K. The results of an electron probe traverse across ALSP1 are compared to these condensation calculations in Fig. 8. The composition of the interior zone of the ALSP1 spinel closely matches that of the spinel predicted to condense from 1780 to 1770 K in terms of their Al, Mg, Cr, and Fe contents. Further along the traverse, as Cr-rich and Cr-poor layers are encountered, the trend is not consistent with equilibrium condensation under the conditions considered here. We did not attempt to model the oscillatory zoning. The data from the traverse also diverge from the predicted Mg and Fe trends, probably due to secondary addition of FeO to the spinel. The calculated spinel compositions do not have high FeO contents despite the relatively oxidizing conditions.

It may be that a period of condensation during slow cooling in a dust-enriched environment such as the one considered here, with fluctuations in temperature and f_{O_2}, could account for the observed Cr_2O_3 zoning pattern in the ALSP1 spinel. At some point the spinel entered an environment in which it was not stable and some resorption took place. The grain was then broken. The smoothness of the fracture surface suggests that the grain did not undergo any significant corrosion after fragmentation.

The condensate Cr-bearing spinel is predicted to co-condense with forsterite, but the O-isotopic data show that the forsterite found in ALSP1 cannot represent that material. The spinel and olivine in ALSP1 formed in different isotopic reservoirs, separated in space, time, or both. They could have formed at the same time, in different parts of an isotopically heterogeneous nebula, or the nebula could have been more ^{16}O-rich when the olivine formed than when the spinel formed. There is abundant evidence that CAIs were initially ^{16}O-rich and were later exposed to a relatively ^{16}O-poor vapor (Clayton, 1993). If the nebula were indeed initially ^{16}O-rich and then became ^{16}O-poor, this would imply that the forsterite in ALSP1 formed before the spinel.

The O-isotopic compositions of the olivine grains in ALSP1 are similar to those of isolated forsterite grains (Weinbruch *et al.*, 1993; Leshin *et al.*, 1998), as are the major and minor element contents of their cores (cf., Steele, 1986). Although grains with compositions like these can be found in chondrules, they are generally interpreted as relic (Jones *et al.*, 1998). These observations are consistent with the formation of olivine as individual grains, perhaps by condensation (Steele, 1986), rimming of the grains, and then assembly into ALSP1, after corrosion and fragmentation of the spinel grain. The nepheline-bearing matrix between olivine grains may represent altered mesostasis, possibly reflecting melting of a small amount of dust that had adhered to the olivine grains.

Formation of ALSP11A

This object exhibits several similarities to ALSP1. Like the latter, it consists of a large spinel grain enclosed in finer-grained olivine that has Mg-rich cores and Fe-rich rims; and there are

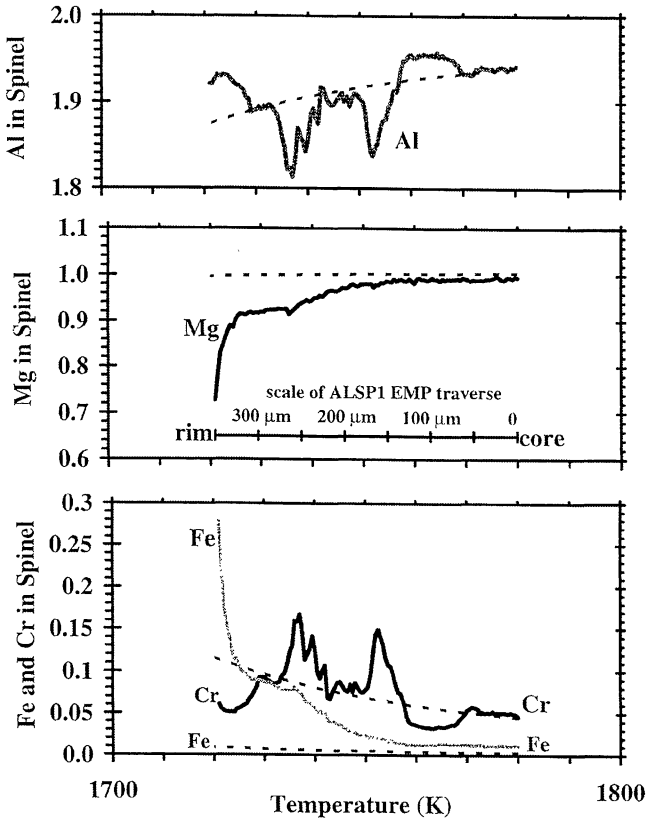

FIG. 8. Abundances of major cations per four O anions in a core–rim electron probe traverse of ALSP1 spinel (solid line) and compositions of spinel predicted to condense (dashed line) at equilibrium from a vapor with a P^{tot} of 10^{-3} bar and a C1-dust/gas ratio of 100× solar. There is a striking similarity between the composition of the core of the spinel and that predicted to condense from 1780 to 1770 K. We did not attempt to model the reversals in Cr-Al zoning.

isotopic differences, in this case between the olivine rims on one hand and the olivine cores and spinel on the other, that show the presence of two components that did not form from the same source. The coarse spinel in this sample has a more Cr_2O_3-rich (50 wt%) chemical composition than the others considered here or that have been found in Murchison (Simon *et al.*, 1994). Its isotopic composition appears to be unusual as well, in that it is ^{16}O-rich compared to the other samples and, although several Murchison samples plot just within error of the CAI line, the spinel in ALSP11A plots on the line, making it unique among Cr-bearing spinel. The coarse spinel and olivine cores have similar O-isotopic compositions to each other and may have formed from a single reservoir, and the olivine rims from another.

If the inclusion ALSP11A crystallized from a melt, then there are two possible explanations for the contrasting isotopic compositions of the spinel and Mg-rich olivine on the one hand and the Fe-rich olivine on the other. The olivine could have undergone subsolidus isotopic exchange with a relatively ^{16}O-poor vapor while the spinel retained its original composition, as in the model inferred for CAIs (Clayton *et al.*, 1977). The other possibility is that the putative FeO-rich liquid from which the FeO-rich olivine might have crystallized could have equilibrated with an ^{16}O-poor vapor, analogous to the process suggested to account for the compositions of a suite of barred chondrules from Allende that are ^{16}O-poor compared to other chondrules from carbonaceous chondrites

(Clayton *et al.*, 1983). It has been suggested (McSween, 1985) that, because they are more FeO-rich, the barred chondrules would have had lower melting points and undergone more extensive melting than other chondrules, and they therefore underwent more complete isotopic exchange than other chondrules, obtaining their present ^{16}O-poor compositions while molten. Inclusion ALSP11A, however, has a porous texture unlike the compact textures of chondrules. Because its cavities are lined with euhedral olivine crystals (Fig. 1f), it is unlikely that they are simply artifacts. If the cavities were formed by a secondary alteration process, we would expect to find alteration products in them but do not. We therefore interpret the voids as a primary feature, one that argues against any model that includes a molten stage. Furthermore, derivation of the spinel in ALSP11A from a chondrule would require that the grain was removed from its host cleanly, without attached phases, and without extensive fracturing, preserving its smooth crystal faces. This seems very difficult, if not impossible, to achieve.

Alternatively, Weinbruch *et al.* (1993) showed that FeO-rich rims of isolated forsteritic olivine grains are ^{16}O-poor relative to their cores, and they concluded that the rims condensed onto the grains, rather than reflecting diffusional exchange of O. It is plausible that ALSP11A was a fluffy aggregate that was so porous that ^{16}O-poor vapor readily infiltrated it and deposited FeO-rich, ^{16}O-poor olivine on the magnesian, relatively ^{16}O-rich olivine grains. The object never melted, retaining its porosity and its unequilibrated isotopic compositions.

There do not appear to be any conditions under which a spinel as Cr-, Fe-rich as that in ALSP11A would condense directly from the nebular gas. Such a spinel could form by reaction of a condensate liquid with the surrounding gas, but only in highly dust-enriched systems. For example, calculations (Ebel and Grossman, 2000) show that spinel nearly as Fe-rich as that in ALSP11A but richer in Cr is stable from 1700 to 1420 K at a P^{tot} of 10^{-3} bar and a dust/gas enrichment of 1000× relative to solar. A spinel like that in ALSP11A would stably coexist with a Cr-bearing liquid and olivine (Fo_{72}) at ~1420 K and the conditions given above. The cores of the large olivine grains in ALSP11A are more Mg-rich than the calculated composition, however. It appears that if the spinel in ALSP11A is a condensate, then the phases predicted to co-condense with it did not accompany it into the final assemblage, as is the case for ALSP1.

The present work confirms that Cr-bearing spinel from both Murchison and Allende is isotopically distinct from CAI-derived, Cr-poor spinel in those meteorites, which plot on the CAI line and are among the most ^{16}O-rich materials known. The spinel in ALSP11A may be indicative of a third population, one that is somewhat Cr- and ^{16}O-enriched and plots on the CAI line.

Chondrules

The unequilibrated isotopic compositions within ALSP1 and ALSP11A contrast with the more homogeneous compositions observed in the petrographically identified chondrules ALSP4, ALSP14A, and Red Eye. The olivine and spinel in ALSP14A are corroded and may have been unstable in their relatively SiO_2-rich host, but they are not isotopically distinct from it. In the other chondrules, the spinel appears to have crystallized *in situ*, and it is not surprising that its isotopic composition is similar to that of the coexisting silicates.

The isotopic compositions of these chondrules are like some previously reported from Allende (Clayton *et al.*, 1983), indicating that the Cr-spinel-bearing chondrules do not have a unique source. That the isotopic composition of ALSP1 spinel is like those of Cr-rich spinels from chondrules indicates that O-isotopic compositions cannot be used to distinguish whether grains from unequilibrated objects are condensates or are fragments from a previous generation of chondrules.

Implications for Chromium Spinels from Murchison and Allende

The spinel in ALSP1 has many characteristics in common with spinels separated from Murchison: zoning; major and minor element abundances; the presence of Al-diopside inclusions; and O-isotopic compositions. It does not fall within the size range of the recovered Murchison grains, being larger by a factor of ~3 than the largest ones, but many of the Murchison grains, like ALSP1, are fragments of once larger crystals, and we therefore do not know their original sizes. Another difference is that the outer margins of the spinel in ALSP1 are more FeO-rich than most of the spinels studied by Simon *et al.* (1994), probably due to a secondary addition of FeO not experienced by the Murchison grains. One chevron-zoned grain from Murchison—SP49 of Simon *et al.* (1994)—shows a slight core-to-rim increase in FeO contents, but others in the Murchison suite do not.

There are also strong similarities between patchy spinels from Allende and Murchison with respect to texture, minor element contents, and O-isotopic compositions. Several of the Allende samples are more FeO-rich than those found in Murchison. These Allende samples were found *in situ*, and they occur as late-crystallizing (*i.e.*, after olivine) phases in ferromagnesian chondrules. Previously, Simon *et al.* (1994) thought it unlikely that patchy spinels could form in chondrules, because that seemed to require that at least two spinel compositions were simultaneously crystallizing from one liquid. Having now observed them *in situ* in chondrules, we must conclude that patchy spinel can be derived from chondrules. The problem of crystallizing multiple compositions of spinel, within single crystals and without any apparent core–rim relationships or crystallographic control remains, however. Exsolution due to miscibility gaps at low temperatures (<700 °C) does not account for the observed patchy spinel, because almost all analyses plot on the Mg-rich, Cr-poor sides of the gaps; the Cr-rich (Cr/(Cr + Al) >0.6) spinel that would be complementary to exsolved Cr-poor spinel (Sack and Ghiorso, 1991) is not observed. Also, the patchy texture is not like any exsolution texture known for spinel (*e.g.*, Haggerty, 1976). Perhaps patchy grains can form in chondrules by crystallization of additional spinel in cavities and embayments in corroded, relic spinel grains.

From our observations of both Red Eye and ALSP4, it is apparent that spinel of more than one zoning type can be present within a single chondrule. We therefore cannot infer that different zoning patterns reflect strongly contrasting thermal histories. Because the chondrule-derived spinel grains tend to be late-crystallizing phases, it may be that their zoning patterns, rather than reflecting specific sources or cooling histories, instead reflect local equilibria with late, relatively low-temperature, isolated liquids, and/or quenching effects.

From their many similarities in addition to their zoning patterns, we conclude that the Cr-bearing spinels in Murchison and Allende were derived from similar sources, with similar bulk chemical and O-isotopic compositions. It appears that many of the Murchison spinels could have been derived from chondrules. If so, then the chemical and isotopic similarities between Mg-rich, Fe-poor ferro-

magnesian chondrules in Allende and Murchison could account for the similarities of the spinel populations. The chevron-zoned grains, for which gas–solid condensation, rather than derivation from chondrules, seems most likely, remain the exception, and they may be representative of a population of condensate grains that was sampled by both Allende and Murchison.

CONCLUSIONS

(1) The chemical compositions, zoning, and O-isotopic compositions of Allende Cr-bearing spinels are similar to those from Murchison, implying similar sources and conditions of formation.

(2) Most zoning types, including patchy, are found in chondrules, with olivine and spinel in apparent O-isotopic equilibrium.

(3) Chevron-zoned spinels are probably gas–solid condensates. At least one from Allende occurs in an olivine-rich object, ALSP1, that may never have been molten.

(4) In both Allende and Murchison, the Mg-, Al-rich, ^{16}O-enriched spinel of CAIs is isotopically distinct from the coarse-grained, Cr-bearing spinel, that has O-isotopic compositions close to those measured for whole chondrules and components of chondrules from carbonaceous chondrites.

(5) Inferred condensate spinel has O-isotopic compositions indistinguishable from those of spinels in chondrules. Condensate grains did not sample a unique reservoir, and the compositions of grains in isotopically unequilibrated objects such as ALSP1 cannot be used to determine whether the grains are condensates or are from a previous generation of chondrules.

Acknowledgments–We are very grateful to Mr. Stephan Kambach for allowing us to section and study ALSP1. We also thank G. Huss and G. J. Wasserburg for the loan of the Red Eye sections, and I. D. Hutcheon for making us aware of the sample. C. Palenik assisted in the petrographic documentation of the samples, and I. M. Steele with cathodoluminescence imaging. The comments of three reviewers and the associate editor led to improvements in the text. This work was supported by NASA through grants NAG5-4476 (L. G.) and NAG5-4704 (K. D. M.), and funding is gratefully acknowledged. The UCLA ion microprobe laboratory is partially supported by a grant from the National Science Foundation Instrumentation and Facilities program.

Editorial handling: D. W. Mittlefehldt

REFERENCES

ALLEN J. M., GROSSMAN L., DAVIS A. M. AND HUTCHEON I. D. (1978) Mineralogy, textures and mode of formation of a hibonite-bearing Allende inclusion. *Proc. Lunar Planet. Sci. Conf.* **9th,** 1209–1233.

CLAYTON R. N. (1993) Oxygen isotopes in meteorites. *Ann. Rev. Earth Planet. Sci.* **21,** 115–149.

CLAYTON R. N. AND MAYEDA T. K. (1984) The oxygen isotope record in Murchison and other carbonaceous chondrites. *Earth Planet. Sci. Lett.* **67,** 151–161.

CLAYTON R. N., ONUMA O., GROSSMAN L. AND MAYEDA T. K. (1977) Distribution of the pre-solar component in Allende and other carbonaceous chondrites. *Earth Planet. Sci. Lett.* **34,** 209–224.

CLAYTON R. N., ONUMA N., IKEDA Y., MAYEDA T. K., HUTCHEON I. D., OLSEN E. J. AND MOLINI-VELSKO C. (1983) Oxygen isotopic compositions of chondrules in Allende and ordinary chondrites. In *Chondrules and Their Origins* (ed. E. A. King), pp. 37–43. Lunar and Planetary Institute, Houston, Texas, USA.

EBEL D. S. AND GROSSMAN L. (2000) Condensation in dust-enriched systems. *Geochim. Cosmochim. Acta* **64,** 339–366.

EILER J. M., GRAHAM C. AND VALLEY J. W. (1997) SIMS analysis of oxygen isotopes: Matrix effects in complex minerals and glasses. *Chem. Geol.* **138,** 221–244.

HAGGERTY S. E. (1976) Opaque mineral oxides in terrestrial igneous rocks. In *Oxide Minerals, MSA Short Course Notes, Vol. 3* (ed. D. Rumble III), pp. Hg-101–Hg-300. Mineralogical Society of America, Washington, D.C., USA.

IRELAND T. R., ZINNER E. K., FAHEY A. J. AND ESAT T. M. (1992) Evidence for distillation in the formation of HAL and related hibonite inclusions. *Geochim. Cosmochim. Acta* **56,** 2503–2520.

JONES R. H. (1992) On the relationship between isolated and chondrule olivine grains in the carbonaceous chondrite ALHA77307. *Geochim. Cosmochim. Acta* **56,** 467–482.

JONES R. H., SAXTON J. M., LYON I. C. AND TURNER G. (1998) Oxygen isotope analyses of chondrule and isolated olivine grains in the CO3 chondrite, ALHA77307 (abstract). *Lunar Planet. Sci.* **29,** #1795, Lunar and Planetary Institute, Houston, Texas, USA (CD-ROM).

LESHIN L. A., MCKEEGAN K. D., ENGRAND C., ZANDA B., BOUROT-DENISE M. AND HEWINS R. H. (1998) Oxygen-isotopic studies of isolated and chondrule olivine from Renazzo and Allende (abstract). *Meteorit. Planet. Sci.* **34 (Suppl.),** A93–A94.

MCKEEGAN K. D., LESHIN L. A., RUSSELL S. S. AND MACPHERSON G. J. (1998) Oxygen isotopic abundances in calcium-aluminum-rich inclusions from ordinary chondrites: Implications for nebular heterogeneity. *Science* **280,** 414–418.

MCSWEEN H. Y., JR. (1985) Constraints on chondrule origin from petrology of isotopically characterized chondrules in the Allende meteorite. *Meteoritics* **20,** 523–539.

POUCHOU J. L AND PICHOIR F. (1984) A new model for quantitative x-ray microanalysis. Part I: Application to the analysis of homogeneous samples. *Rech. Aerosp.* **3,** 13–38.

RUSSELL S. S., LESHIN L. A., MCKEEGAN K. D. AND MACPHERSON G. J. (1998) Oxygen-16 enrichments in aluminum-rich chondrules from unequilibrated ordinary chondrites (abstract). *Lunar Planet. Sci.* **29,** #1826, Lunar and Planetary Institute, Houston, Texas, USA (CD-ROM).

SACK R. O. AND GHIORSO M. S. (1991) Chromian spinels as petrogenetic indicators: Thermodynamics and petrological applications. *Am. Mineral.* **76,** 827–847.

SIMON S. B., GROSSMAN L., PODOSEK F. A., ZINNER E. AND PROMBO C. A. (1994) Petrography, composition, and origin of large, chromian spinels from the Murchison meteorite. *Geochim. Cosmochim. Acta* **58,** 1313–1334.

SIMON S. B., GROSSMAN L., EBEL D. S. AND PALENIK C. (1998) Large, relict chromian spinels in Allende: A link to Murchison? (abstract). *Lunar Planet. Sci.* **29,** #1640, Lunar and Planetary Institute, Houston, Texas, USA (CD-ROM).

SIMON S. B., MCKEEGAN K. D. AND GROSSMAN L. (1999) Oxygen isotopic compositions of Cr-spinel-bearing objects in Allende (abstract). *Meteorit. Planet. Sci.* **34 (Suppl.),** A108–A109.

STEELE I. M. (1986) Compositions and textures of relic forsterite in carbonaceous and unequilibrated ordinary chondrites. *Geochim. Cosmochim. Acta.* **50,** 1379–1395.

STEELE I. M. (1992) Olivine in Antarctic micrometeorites: Comparison with other extraterrestrial olivine. *Geochim. Cosmochim. Acta* **56,** 2923–2929.

STEELE I. M. AND SMITH J. V. (1986) Contrasting forsterite compositions for C2, C3 and UOC meteorites (abstract). *Lunar Planet. Sci.* **17,** 822–823.

WEINBRUCH S., PALME H., MÜLLER W. F. AND EL GORESY A. (1990) FeO-rich rims and veins in Allende forsterite: Evidence for high temperature condensation at oxidizing conditions. *Meteoritics* **25,** 115–125.

WEINBRUCH S., ZINNER E., EL GORESY A., STEELE I. M. AND PALME H. (1993) Oxygen isotopic composition of individual olivine grains from the Allende meteorite. *Geochim. Cosmochim. Acta.* **57,** 2649–2661.

YONEDA S. AND GROSSMAN L. (1995) Condensation of CaO-MgO-Al_2O_3-SiO_2 liquids from cosmic gases. *Geochim. Cosmochim. Acta.* **59,** 3413–3444.